This is a pre-print of an article published in *Journal of Superconductivity and Novel Magnetism*. The final authenticated version is available online at: https://doi.org/10.1007/s10948-017-3996-6

Shape-anisotropic nickel-PDMS composites with uniaxial magnetic anisotropy obtained by emulsification under magnetic field

J.G. Cabal-Velarde[a,b], A.L. Guerrero[c], E. Romero-Tela[c], J.H. García-Gallegos[d], J.L. Sánchez Llamazares[b], A. Encinas[b,*]

[a]*Instituto Tecnológico Superior de Irapuato, Carretera Irapuato-Silao Km 12.5, 36821, Irapuato, Guanajuato, México.*
[b]*División de Materiales Avanzados, Instituto Potosino de Investigación Científica y Tecnológica A.C., Camino a La Presa de San José 2005, 78216. San Luis Potosí, S.L.P., México.*
[c]*Facultad de Ciencias, Universidad Autónoma de San Luis Potosí, Av. Manuel Nava 6, Zona Universitaria, 78290, San Luis Potosí, S.L.P., México.*
[d]*Universidad Tecnológica de San Juan del Río Querétaro, División de Energías Renovables Av. La Palma No. 125, Vista Hermosa, 76800, San Juan del Río, Querétaro, México.*

Abstract. Magnetic microcomposites were fabricated by emulsification of a mixture of polydimethylsiloxane (PDMS) and nickel microparticles. The composites were obtained in a temperature controlled water-surfactant media with and without the influence of an external magnetic field. The presence of a moderate external magnetic field of 80 G (8 mT) during the polymerization stage leads to the arrangement of nickel microparticles into chains that form the magnetic core of the synthesized composites. The method allows to control the shape of the composite particles by applying a magnetic field and varying the stirring speed. Three shapes of composite particles, namely, spherical, teardrops and ellipsoidal were obtained and magnetically characterized. Room temperature hysteresis loops and d*M*/d*H* versus *H* curves in the second-to-third quadrants show that spherical particles are isotropic while non-spherical particles show an induced uniaxial magnetic anisotropy which depends on the shape of the resulting composite particles.

Keywords: magnetic elastomers; composite materials; anisotropic composites.

* Corresponding author. Email address: armando.encinas@ipicyt.edu.mx

1. Introduction

Magnetic elastomers have emerged as a new class of two-component composites consisting of small magnetic particles embedded or coated in a polymeric matrix [1, 3]. Combination of a magnetic material in the form of particles with the properties of a polymer potentially opens their use in actuators for aerospace and automotive applications [4-6], microelectromechanical systems (MEMS) [1, 7-8] and microfluidic valves [9-11]. In the field of medicine these composites also may have relevant potential applications for cancer treatment therapy [12-13] and controlled drugs delivery [14]. The combination of magnetic properties with those of the polymeric matrix leads to various functionalities which can be triggered by applying an external magnetic field; examples of that are the shape memory effect [15], or the magnetostrictive and elastomagnetic phenomena [16-17]. Therefore, the recent interest in this new class of functional materials encourages basic research aimed to develop novel technology. Polydimethylsiloxane (PDMS), which is a biocompatible type of silicone rubber with hydrophobic and oleophobic properties [18], is one of the most promising elastomers for this purpose that it can be used in a wide range of applications. In addition, PDMS has several other advantageous properties such as high dielectric strength, compressibility, gas permeability, flexibility, chemically unreactive, and low curing temperature [19-21]. At last, it is commercially available at a low-cost, is recyclable and usable over a wide temperature range (from -100 °C to 100 °C) [22-23]. However, the magnetic behavior and physical properties of the PDMS-based magnetic composites have been less explored [1].

Magnetic polymer composites are currently of great interest since they allow a non-contact remote control using an externally applied magnetic field. The most direct approach to fabricate these composites is by embedding the magnetic particles in elastomers. This allows the use of a magnetic field during polymerization to induce the formation of chains of particles inside the elastomer, and once the polymerization is complete, these chains remain embedded in the composite [24]. The chains form due to the dipole-dipole interaction leading to an uniaxial magnetic anisotropy [25]. This type of dipolar magnetic anisotropy in particle chains is the same used by magnetotactic bacteria to produce a magnetic compass [26]. Uniaxial magnetic anisotropy is a fundamental property in magnetic responsive materials since it provides an easy and a hard magnetization axes; in this case, the material displays a more complex behavior than the exhibited by an isotropic composite. In this contribution, we present a fabrication procedure that combines emulsification of an elastomer with dispersed magnetic micro-particles under the application of an external magnetic field to induce the formation of magnetic particle chains during polymerization. The novelty of our study is threefold: first, a simple method is presented to fabricate shape-anisotropic microparticles; second, in non-spherical particles, a uniaxial magnetic anisotropy is induced by the fabrication process, and; third, the fabrication method is based on emulsification which is a scalable method for the production of colloidal particles.

2. Experimental section

PDMS based microcomposites were prepared using PDMS (Sylgard 184) with a monomer-to-crosslinker weight ratio of 10:1. As magnetic filler, we used commercially available 99.999 % pure nickel powder from Sigma-Aldrich with a particle size < 150 μm. In order to reduce the average particle size, nickel powder was mechanically milled during 2 hours at 90 rpm by using a ball mill from U.S. Stoneware.

Composites were produced by the microemulsion method from a mixture of 70% wt. of PDMS and 30% wt. of milled nickel particles. The blend was homogenized during 20 minutes in an ultrasonic bath, whereas air bubbles were dynamically extracted using a vacuum pump during 10 minutes. A schematic representation of the experimental setup used to synthesize the two-component microcomposites is shown in Fig. 1. 40 ml of a commercially available surfactant was added at room temperature to 5 ml of the PDMS-Ni dough under continuous stirring with a Cole Parmer stir-pack general laboratory mixer. The stirrer blades were disks of propylene with several randomly distributed micro-holes; the experimental setup used had five blades evenly spaced along of a mounting rod. The diameter of the blades is slightly smaller than the diameter of the glass test tube used to contain the surfactant. The microemulsion system was submerged in a water bath while the temperature increased at 3 °C/min up to a the polymerization temperature of 90 °C. A solenoidal coil made of copper wire was wound around the outer part of the water bath; the axial external magnetic field applied during the polymerization process align nickel microparticles inside the PDMS body.

The magnetic field produced by the handmade solenoidal coil at the center of the glass test tube was measured by using a F.W. Bell model 5180 Gaussmeter. With a

stirring speed of 2000 rpm, samples were prepared under a static magnetic field of 80 G (8 mT) and without magnetic field. The effect of stirring speed during emulsion polymerization under constant magnetic field (B = 80 G) was also tested in a third sample, wherein the rotation speed was reduced by 80 %.

Milled nickel particles were characterized by X-ray diffraction in a Bruker AXS model D8 Advance diffractometer with CuKα radiation ($40° \leq 2\theta \leq 80°$; step increment 0.02°). The Rietveld refinement on the XRD pattern was carried out with the MAUD program [27]. Magnetic characterization of both, the nickel particles and the composites was performed by means of the major hysteresis loops obtained from a Micromag 2900 alternating gradient magnetometer. Analysis of the shape, morphology and size of nickel particles and composites were examined by scanning electron microscopy (SEM); SEM micrographs were obtained using a FEI Philips XL30 sFEG scanning electron microscope.

3. Results and discussion

Fig. 2(a) shows the experimental and calculated X-ray diffractogram of milled nickel particles; no traces of secondary phases were observed. The initial refinement model considers a cubic closed-packed crystal structure with Fm-3m space group and a cell parameter a = 3.524 Å. From the refinement, we obtained a cell parameter of a = 3.5238 ± 0.0006 and an average crystallite size of 244 ± 8 nm.

The SEM micrographs of the nickel particles after grinding are presented in Fig. 2(b) and (c). Nickel particles present irregular shapes with sharp edges and tend to form spherical agglomerates with an average size of 4 μm. It must be also noted that

after 2 hours of milling, the grain size of particles (initially below 150 μm), was considerably reduced (~ 97 %).

Fig. 3(a) shows the SEM micrograph of PDMS-Ni composite prepared from the microemulsion method in the absence of an external magnetic field at a stirring speed of 2000 rpm. Note that composites acquire a spherical shape and their surface incorporate small bulges of the polymeric material. By varying the stirring speed from 400 to 2000 rpm the particles obtained were spherical in shape.

In a second experiment, the stirring speed was kept at 2000 rpm and the external magnetic field of 80 G (8 mT) is applied. So, the polymerization process takes place under the presence of the field. As shown in Fig. 3(b) at this stirring speed microcomposites particle shape changes from spherical to teardrops. These results suggest that the resulting microcomposite particle shape may change by properly combining stirring speed magnetic field during the polymerization process. Stirring leads to particle rotation in the horizontal plane, while the magnetic field acts perpendicular to this plane; because of the centrifugal force effect, in this configuration nickel particles are slowly pulled to the back part of the composite adopting the teardrop shape. In a further experiment, the stirring speed was reduced to 400 rpm maintaining constant the external applied magnetic field (80 G), the centrifugal entrainment of nickel particles forming the composite diminishes reinforcing their trend to align parallel to the field. As a result, nickel particles wrapped by the polymer do not accumulate in one end of the composite capsule and after completion of polymerization the resulting composite acquires an ellipsoidal shape, as Fig. 3(c) shows.

To perform the magnetic characterization, the particles of the three fabricated composites were oriented by applying a homogeneous magnetic field of 50 G (5 mT) and fixed in a PDMS matrix prior to their measurement. Fig. 4 shows their hysteresis loops measured applying the external magnetic field along two orthogonal directions (i.e., the long and short axes, respectively); in the graphs, the magnetization axis has been normalized by its maximum value to emphasize on the differences. Fig. 4(a) compares the hysteresis loops of the as-milled nickel particles and the synthesized spherical microcomposite particles. In this case, the hysteresis loops measured parallel and perpendicular to the orientation direction overlap, so, the magnetic properties of composite particles match with that nickel and do not depend on magnetic field direction. They are isotropic. Fig. 4(b) shows that the magnetization of teardrop shape composite particles depends of the magnetic field direction with respect to the composite axes. When field is applied through the short axis, the saturation is reached at 4.19 kOe; in contrast, when it is applied field along to the long axis, the saturation is obtained at a lower field. Ellipsoidal shape samples shown in Fig. 4(c) have a similar behavior than the teardrop shape samples but with slight differences in their magnetization values, as Table I shows. They show similar coercivity and remanent-to-saturation (M_r/M_S) values. Noting that a higher remanence is found along the longest axis in the non-spherical particles. The most significant differences are observed in the saturation magnetic field. The results clearly show that the particles have uniaxial magnetic anisotropy with the easy magnetization axis oriented parallel to their longer axis. This uniaxial anisotropy comes from the Ni particle chains induced by the magnetic field during

polymerization. This type of dipolar chains are well known to result in a uniaxial magnetic anisotropy [25]

Fig. 5 shows the d*M*/d*H* vs *H* curves, or switching field distribution (SFD), obtained from the first derivative of the demagnetizing curve. Fig. 5(a) and (b) show the SFD along the long and short axes of the composite particles with teardrop and ellipsoidal shapes, respectively. The effect of the induced magnetic anisotropy due the particle chains is clearly observed. Both plots show a significant broadening when the magnetic field is applied through the short axis, owing to the magnetic field is applied along the hard axis [28]. (c) and (d) compares the SFD obtained along the short and long axes for teardrops and ellipsoidal microcomposite particles with the one obtained for isotropic spherical ones. Along the long axis, these curves are narrower with respect to those shown by the spherical composites, because of the field is applied along the easy axis. Teardrops and ellipsoidal composites show hard and easy magnetization directions along their short and large axes, respectively; accordingly, the magnetization behavior varies when the magnetic is applied along these principal directions.

4. Conclusion

In conclusion, we have shown that combining a low intensity magnetic field with a simple and scalable technique, such as emulsification, it is possible to produce both shape-anisotropic and magnetically anisotropic micro-composite PDMS-Ni particles. Regarding their shape, the composites can be spherical, ellipsoidal or teardrop shaped. In non-spherical composites a

uniaxial magnetic anisotropy is obtained which is attributed to the Ni particle chains induced during polymerization by the applied magnetic field. The shape and uniaxial magnetic anisotropy in the developed composites can be of potential interest for their applications in remotely controlled colloidal composites.

Acknowledgment

This work was supported by CONACYT Mexico (scholarship 164229; ERT), as well as by the agreements PROMEP-02/Rev-06 (JGCV) and PRODEP/103.5/13/10573 (JHGG). The authors acknowledge the support received from Laboratorio Nacional de Investigaciones en Nanociencias y Nanotecnología (LINAN, IPICYT).

References

[1] H. Denver, T. Heiman, E. Martin, A. Gupta, D.A. Borca-Tasciuc, Fabrication of polydimethylsiloxane composites with nickel nanoparticle and nanowire fillers and study of their mechanical and magnetic properties, J. Appl. Phys. 106 (2009) pp. 064909 (doi:10.1063/1.3224966)

[2] S. Abramchuk, E. Kramarenko, D. Grishin, G. Stepanov, L.V. Nikitin, G. Filipcsei, A.R. Khokhlov, M. Zrínyi, Novel highly elastic magnetic materials for dampers and seals: part II. Material behavior in a magnetic field, Polym. Adv. Tech. 18 (2007) pp. 513-518. (doi: 10.1002/pat.923)

[3] Z. Varga, F. Fehér, G. Filipcsei, M. Zrínyi, Smart nanocomposite polymer gels, Macromol. Symp. 200 (2003) pp. 93. (doi:10.1002/masy.200351009)

[4] M. Balasoiu, M.L. Craus, E.M. Anitas, I. Bica, J. Plestil, A.I. Kuklin, Microstructure of Stomaflex Based Magnetic Elastomers, Phys. Solid State 52 (2010) pp. 917-921. (doi:10.1134/S1063783410050070)

[5] Q. Han, X. Shen, W. Zhu, C. Zhu, X. Zhou, H. Jiang, Magnetic sensing film based on Fe3O4@Au-GSH molecularly imprinted polymers for the electrochemical detection of estradiol, Biosens. Bioelec. 79 (2016) pp. 180-186. (doi:10.1016/j.bios.2015.12.017)

[6] T. Manouras, M. Vamvakaki, Field responsive materials: photo-, electro-, magnetic- and ultrasound-sensitive polymers, Polym. Chem. 8 (2017) pp. 74-96 (doi:10.1039/C6PY01455K)

[7] K.H. Cheah, P.S. Khiew, J.K. Chin, Fabrication of a zirconia MEMS-based microthruster by gel casting on PDMS soft molds, J. Micromech. Microeng. 22 (2012) pp. 09013. (doi: 10.1088/0960-1317/22/9/095013)

[8] A.P. Gerratt, I. Penskiy, S. Bergbreiter, In situ characterization of PDMS in SOI-MEMS, J. Micromech. Microeng. 23 (2013) pp. 045003. (doi:10.1088/0960-1317/23/4/045003)

[9] M. Nagai, M. Soga, T. Miyamoto, T. Kawashima, T. Shibata, MEMS-based dispenser array for selective immobilization of molecular recognition elements on bio-image sensor, 2014 International Symposium on Micro-NanoMechatronics and Human Science (MHS) (2014) (doi:10.1109/MHS.2014.7006138)

[10] M. Farshad, A. Benine, Magnetoactive elastomer composites, Polymer. Testing. 23 (2004) pp. 347-353. (doi:10.1016/S0142-9418(03)00103-X)

[11] A. Terray, J. Oakey, D.M.W. Marr, Microfluidic Control Using Colloidal Devices, Science 296 (2002) pp. 1841-1844. (doi:10.1126/science.1072133)

[12] K.E. Scarberry, E.B. Dickerson, Z.J. Zhang, B.B. Benigno, J.F. McDonald, Selective removal of ovarian cancer cells from human ascites fluid using magnetic nanoparticles, Nanomedicine: Nanotech. Biology and Med. 6 (2010) pp. 399-408. (doi:10.1016/j.nano.2009.11.003)

[13] M.F. Maitz, Applications of synthetic polymers in clinical medicine, Biosurface Biotribology 1 (2015) pp. 161-176. (doi:0.1016/j.bsbt.2015.08.002)

[14] F.N. Pirmoradi, J.K. Jackson, H.M. Burt, M. Chiao, A magnetically controlled MEMS device for drug delivery: design, fabrication, and testing, Lab Chip 11 (2011) pp. 3072-3080. (doi:10.1039/c1lc20438f).

[15] E.Z. Meilikhov, R.M. Farzetdinova, Structural Phase Transitions in Isotropic Magnetic Elastomers, J. Exp. Theor. Phys. 122 (2016) pp. 1038-1046. (doi:10.1134/S1063776116060170).

[16] C.W. Nan, M. Li, Possible giant magnetoelectric effect of ferromagnetic rare-earth–iron-alloys-filled ferroelectric polymers, Appl. Phys. Lett. 78 (2001) pp. 2527-2529. (doi:10.1063/1.1367293)

[17] X. Guan, X. Dong, J. Ou, Magnetostrictive effect of magnetorheological elastomer, J. Magn. Magn. Mater. 320 (2008) pp. 158-163. (doi:10.1016/j.jmmm.2007.05.043)

[18] D. Wu, S. Wu, Q. Chen, S. Zhao, H. Zhang, J. Jiao, J. A. Piersol, J.N. Wang, H.B. Sun, L. Jiang, Facile creation of hierarchical PDMS microstructures with extreme underwater superoleophobicity for anti-oil application in microfluidic channels, Lab Chip 11 (2011) pp. 3873-3879. (doi:10.1039/C1LC20226J)

[19] A. Mata, A. J. Fleischman, S. Roy, Characterization of Polydimethylsiloxane (PDMS) Properties for Biomedical Micro/Nanosystems, Biom. Microd. 7 (2005) pp. 281. (doi:10.1007/s10544-005-6070-2)

[20] B.H. Jo, L.M. Van Lerberghe, K.M. Motsegood, D.J. Beebe, Three-dimensional micro-channel fabrication in polydimethylsiloxane (PDMS) elastomer, J Microelectromech. Syst. 9 (2000) pp. 76. (doi:10.1109/84.825780)

[21] M.W. Toepke, D.J. Beebe, PDMS absorption of small molecules and consequences in microfluidic applications, Lab Chip 6 (2006) pp. 1484-1486. (DOI: 10.1039/B612140C).

[22] J.C. Lotters, W. Olthuis, P.H. Veltink, P. Bergveld, The mechanical properties of the rubber elastic polymer polydimethylsiloxane for sensor applications, J. Micromech. Microeng. 7 (1997) pp. 145. (doi:10.1088/0960-1317/7/3/017)

[23] A. Mata, A.J. Fleischman, S. Roy, Characterization of polydimethylsiloxane (PDMS) properties for biomedical micro/nanosystems, Biomed. Microdevices 7 (2005) pp. 281-293. (doi:10.1007/s10544-005-6070-2)

[24] S. R. Mishra, M. D. Dickey, O. D. Velev, J. B. Tracy, Nanoscale 8 (2016) pp. 1309-1313. (doi: 10.1039/C5NR07410J)

[25] I.S. Jacobs and C.P. Bean, Phys. Rev. 100 (1955) pp. 1060. (doi: https://doi.org/10.1103/PhysRev.100.1060)

[26] R. Uebe, D. Schüler, Nature Rev. Microbiol. 14 (2016) pp. 621–637. (doi:10.1038/nrmicro.2016.99)

[27] L. Lutterotti, S. Matthies, H.R. Wenk, MAUD: a friendly Java program for material analysis using diffraction, IUCr Newsletter of the CPD. 21 (1999) pp. 14.

[28] O. Hellwig, A. Berger, T. Thomson, E. Dobisz, Z.Z. Bandic, H. Yang, D.S. Kercher, E.E. Fullerton, Separating dipolar broadening from the intrinsic switching field distribution in perpendicular patterned media, App. Phys. Lett. 90 (2007) pp. 162516. (doi:10.1063/1.2730744).

FIGURE CAPTIONS

Fig. 1. Schematic representation of the experimental setup used to synthesize the two-components composites by the microemulsion method.

Fig. 2. (a) Experimental (square black symbols) and calculated (continuous red line) X-ray diffraction patterns for as-milled nickel particles. The difference between them is depicted at the bottom of the figure, whereas the green vertical bars indicate the position of Bragg reflections. (b) and (c) SEM micrographs at different magnifications of as-milled nickel particles.

Fig. 3. Typical SEM micrograph of microemulsioned composites particles sinthesized with spherical (a), teardrop (b) and ellipsoidal (c) shapes.

Fig. 4. Room temperature hysteresis loops measured for: (a) nickel powder (black continuous line) and spherical microcomposites (red dots); (b) and (c) teardrops and ellipsoidal microcomposites, respectively, along their long (green circles) and short (blue squares) axes. The hysteresis loop of the spherical microcomposites in (b) and (c) is indicated by the red dots.

Fig. 5. (a) and (b) switching field distribution for teardrop and ellipsoidal microcomposite particles, respectively, along the long (green circles) and short (blue squares) axes. (c) and (d) Comparison of the switching field distribution along the short (c) and long (d) axes for and teardrops (black line) and ellipsoidal (green line) microcomposite particles with the one obtained for isotropic spherical ones (red dots).

TABLE CAPTIONS

Table I. Magnetic properties derived from the room temperature hysteresis loop for the polymer-coated composite particles synthesized.

Table I. Magnetic properties derived from the room temperature hysteresis loop for the polymer-coated composite particles synthesized.

Particle shape	**Axis**	M_r/M_S	**Coercivity** (kOe)	**Saturation magnetic field** (kOe)
Spherical	isotropic	0.040	0.051	4.09
Teardrop	long	0.061	0.051	4.09
	short	0.032	0.051	4.19
Elliptical	long	0.067	0.050	2.74
	short	0.035	0.050	2.99

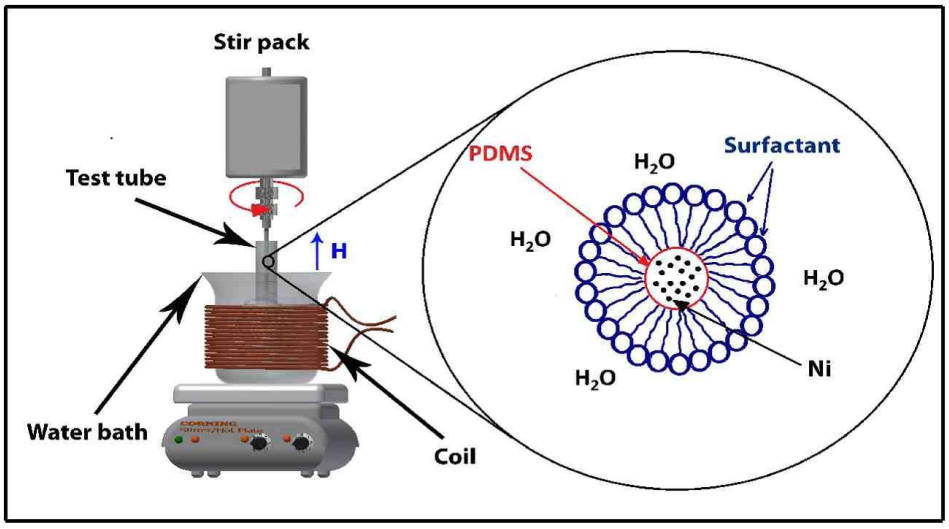

Fig. 1. Schematic representation of the experimental setup used to synthesize the two-components composites by the microemulsion method.

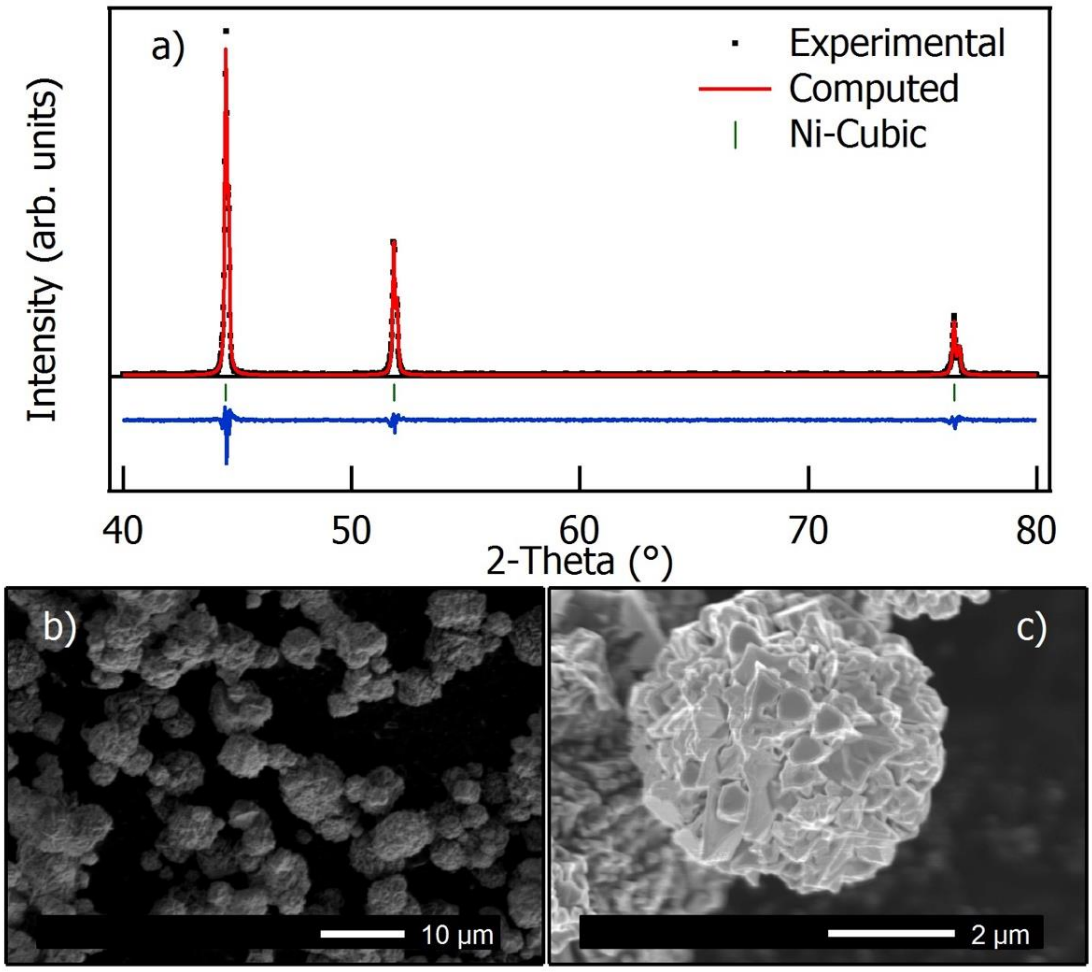

Fig. 2. (a) Experimental (square black symbols) and calculated (continuous red line) X-ray diffraction patterns for as-milled nickel particles. The difference between them is depicted at the bottom of the figure, whereas the green vertical bars indicate the position of Bragg reflections. (b) and (c) SEM micrographs at different magnifications of as-milled nickel particles.

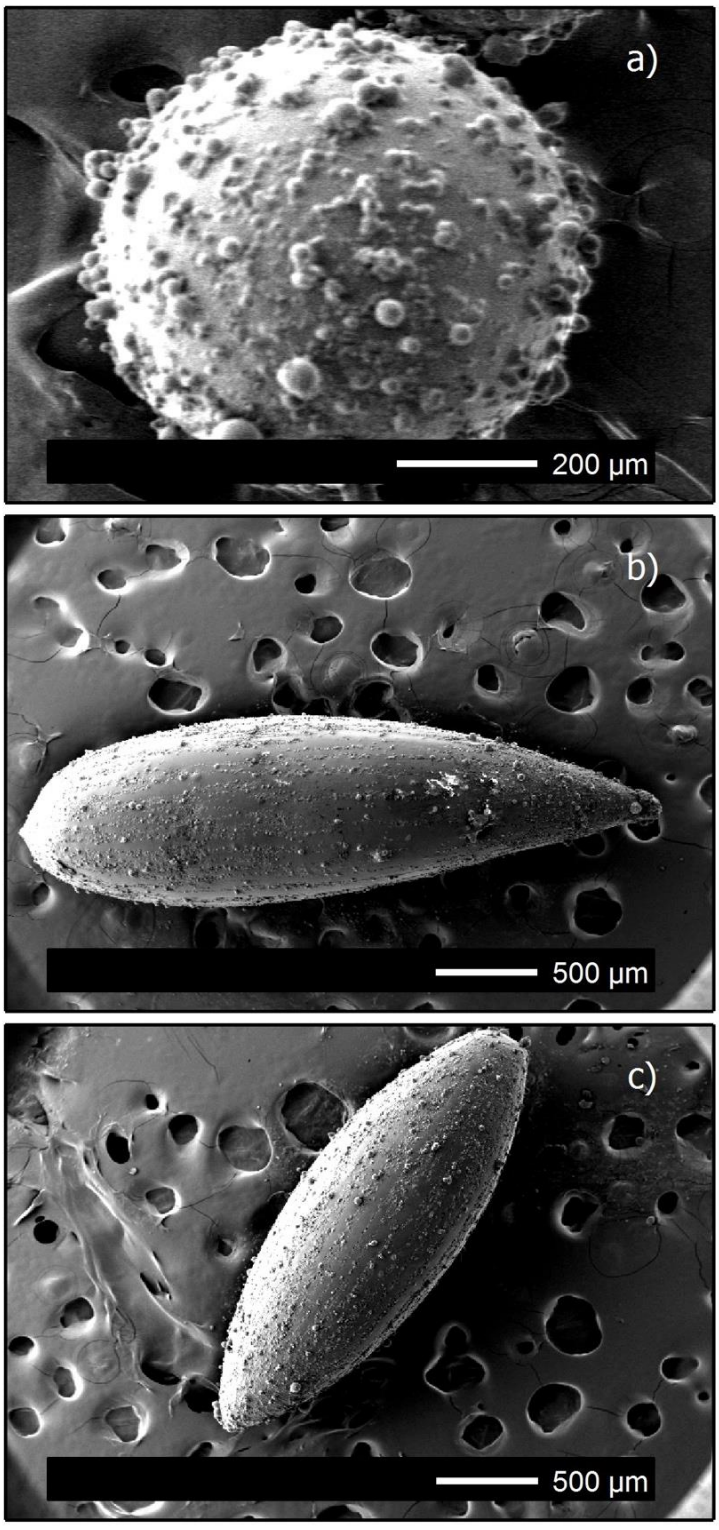

Fig. 3. Typical SEM micrograph of microemulsioned composites particles sinthesized with spherical (a), teardrop (b) and ellipsoidal (c) shapes.

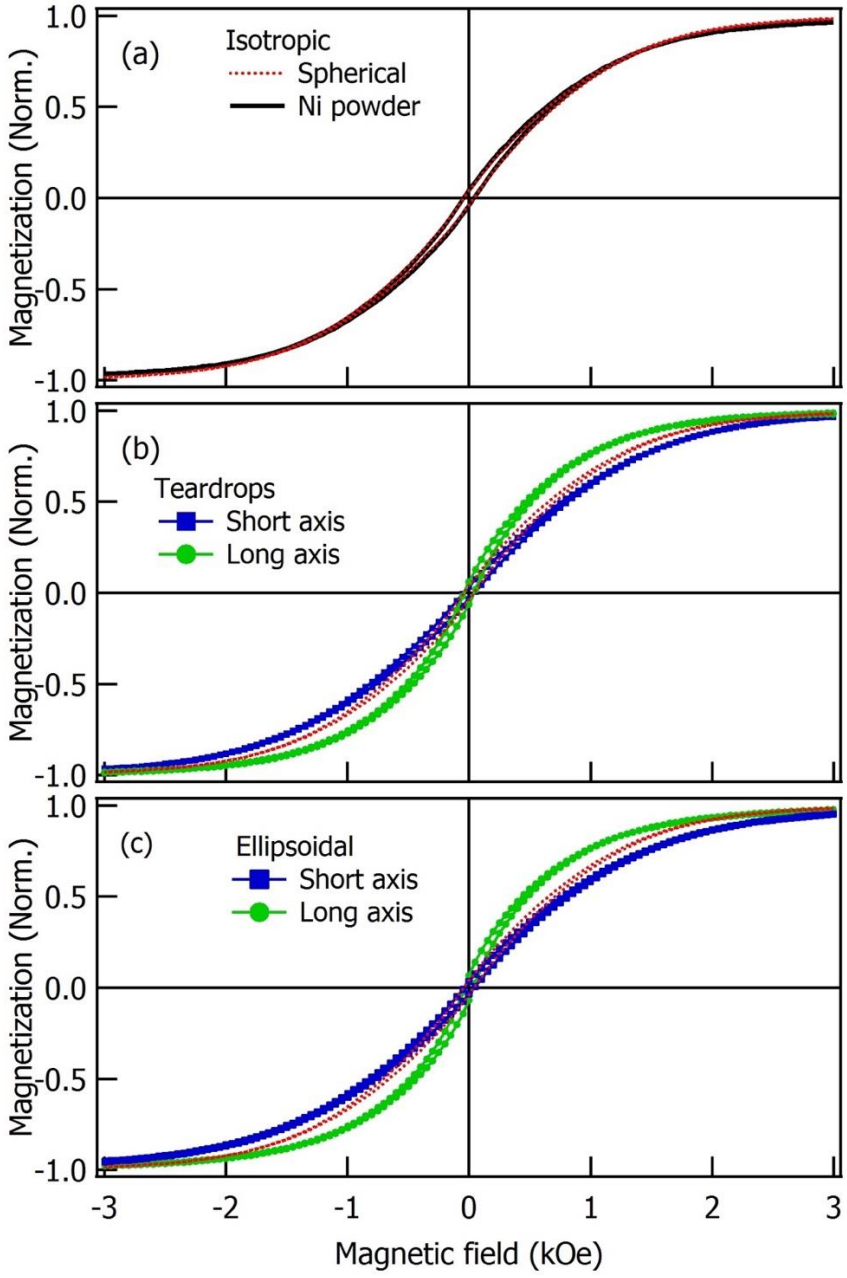

Fig. 4. Room temperature hysteresis loops measured for: (a) nickel powder (black continuous line) and spherical microcomposites (red dots); (b) and (c) teardrops and ellipsoidal microcomposites, respectively, along their long (green circles) and short (blue squares) axes. The hysteresis loop of the spherical microcomposites in (b) and (c) is indicated by the red dots.

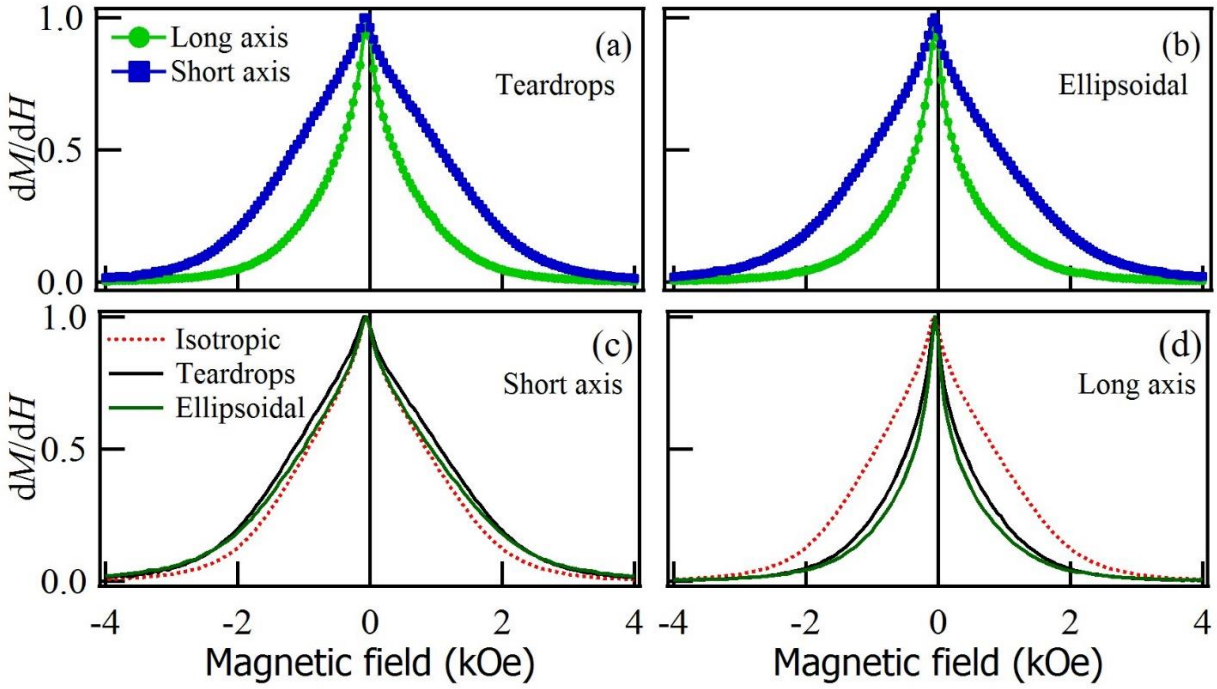

Fig. 5. (a) and (b) switching field distribution for teardrop and ellipsoidal microcomposite particles, respectively, along the long (green circles) and short (blue squares) axes. (c) and (d) Comparison of the switching field distribution along the short (c) and long (d) axes for and teardrops (black line) and ellipsoidal (green line) microcomposite particles with the one obtained for isotropic spherical ones (red dots).